Smooth-Particle Phase Stability with Generalized Density-Dependent Potentials

Wm. G. Hoover and Carol G. Hoover

Highway Contract 60, Box 565

Ruby Valley, Nevada 89833

(Dated: November 7, 2005)

Abstract

Stable fluid and solid particle phases are essential to the simulation of continuum fluids and solids using Smooth Particle Applied Mechanics. We show that density-dependent potentials, such as $\Phi_\rho = \frac{1}{2}\sum(\rho - \rho_0)^2$, along with their corresponding constitutive relations, provide a simple means for characterizing fluids and that special stabilization potentials, with density gradients or curvatures, such as $\Phi_{\nabla\rho} = \frac{1}{2}\sum(\nabla\rho)^2$, not only stabilize crystalline solid phases (or meshes) but also provide a surface tension which is missing in the usual density-dependent-potential approach. We illustrate these ideas for two-dimensional square, triangular, and hexagonal lattices.

PACS numbers: 46.15.-x, 83.85.Pt

Keywords: Smooth Particles, Stability, Density Gradients, Surface Tension

I. SMOOTH PARTICLE APPLIED MECHANICS

Smooth particle applied mechanics—SPAM—was discovered about thirty years ago[1, 2]. It has become a useful tool in simulating gases, fluids, and solids, and holds particular promise for problems involving large high-speed deformation and failure. The main advantage of the method is simplicity. SPAM closely resembles atomistic molecular dynamics and, in a variety of cases[3], the SPAM particle trajectories are isomorphic to those of molecular dynamics.

A smooth-particle code is less-complicated than typical grid-based continuum codes because the smooth-particle method evaluates spatial gradients in a particularly simple way, explained in more detail below. The main disadvantages of the method are instability in tension[4] and the lack of surface tension[5]. The present work introduces an idea—potentials depending upon the local variation of the density—designed to address those problems.

The basic smooth-particle approach is to represent all continuum properties (the density ρ, the velocity v, the stress tensor σ, ...) as interpolated sums of particle properties, where the particles are described by "weight functions", expressing the range of influence of the particles in space. The *simplest* weight function satisfying five desirable conditions—(i) normalization, (ii) finite range h, (iii) a maximum at the origin, and (iv and v) two continuous derivatives everywhere—is Lucy's. Normalized for applications in two-dimensional space Lucy's weight function is as follows:

$$w_{\rm Lucy}(r<h) = \frac{5}{\pi h^2}\left[1-\frac{r}{h}\right]^3\left[1+3\frac{r}{h}\right]$$
$$\longrightarrow \int_0^h 2\pi r w(r) dr \equiv 1 \ .$$

In the present work we will also use an even smoother extension of Lucy's weight function, a normalized weight function with *three* continuous derivatives:

$$w_{\rm Smooth}(r<h) = \frac{7}{\pi h^2}\left[1-\frac{r}{h}\right]^4\left[1+4\frac{r}{h}\right] \ .$$

In any case, the density at a point r is defined as the sum of all the particle contributions at that point:

$$\rho(r) \equiv \sum_j m_j w(r-r_j) \ ,$$

so that the density associated with Particle i is the density evaulated there:

$$\rho_i = \sum_j m_j w_{ij} \ ; \ w_{ij} \equiv w(|r_i - r_j|) = w(r_{ij}) \ .$$

Other continuum properties at location r are likewise calculated as sums over nearby particles:

$$f(r)\rho(r) \equiv \sum_j m_j f_j w(|r - r_j|) \longrightarrow$$

$$f(r) = [f(r)\rho(r)]/\rho(r) =$$

$$\sum_j m_j f_j w(|r - r_j|) / \sum_j m_j w(|r - r_j|) \ .$$

It is important to note that, unlike the density $\rho(r_i) = \rho_i$, the interpolated function $f(r)$ at the location of Particle j is typically different to the particle property f_j at that point, $f(r_j) \neq f_j$.

Beyond using the point properties $\{f_j\}$ to define the field properties $f(r)$ the smooth-particle approach has the crucial advantage that *gradients* of the field properties translate into simple sums of particle quantities:

$$\nabla(\rho f)_r = (f\nabla\rho)_r + (\rho\nabla f)_r \equiv$$

$$\nabla_r \left[\sum_j m_j f_j w(|r - r_j|) \right] = \sum_j m_j f_j \nabla_r w(|r - r_j|) \ .$$

Expressions for the gradients of density, velocity, stress, and energy make it possible to express the *partial* differential equations of continuum mechanics as *ordinary* differential equations for the evolution of the particle coordinates, velocities, stresses, and energies[6]. The resulting "equation of motion" for the particles is

$$\dot{v}_i = -\sum_j \left[(mP/\rho^2)_i + (mP/\rho^2)_j \right] \cdot \nabla_i w_{ij} \ ,$$

where P_i is the pressure tensor associated with Particle i. Where the pressure is hydrostatic, and slowly varying in space, it is noteworthy that the smooth-particle equations of motion are exactly the same as the equations of molecular dynamics, with the weight function $w(r)$ playing the rôle of a pair potential. In the simple case that the internal energy depends only on volume (and not on temperature) the pressure is simply related to the internal energy per unit mass e:

$$P = \rho^2 de/d\rho \ .$$

Specifying the density dependence of either the pressure or the internal energy, in such a case, corresponds to giving a full description of the equilibrium equation of state.

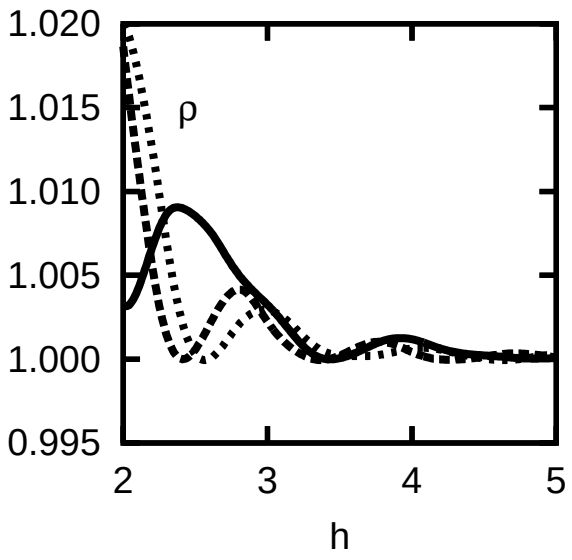

FIG. 1: Summed-up densities evaluated *at* regular-lattice particle sites for (from top to bottom at the left side of the plot) the square, triangular, and hexagonal lattices. The range of Lucy's weight function varies from 2 to 5 where the overall density of the lattice is unity and all the particles have unit mass.

II. CONVERGENCE OF SMOOTH-PARTICLE AVERAGES

The evolving time-and-space dependent smooth-particle sums converge to continuum mechanics as a many-particle limit, just as do the more usual grid-based approximations. The range of the smooth-particle weight function, h, corresponds to a few grid spacings. In practice, for an error level of order one percent, the weight-function sums must include a few dozen particles. Fig. 1 shows the dependence of density sums, $\rho_i = \sum_j m_j w_{ij}$ on the range of the weight function for three regular two-dimensional lattices. In typical applications, with $h \simeq 3\sqrt{V/N}$ the density errors are of order one percent.

The density curves in the Figure correspond to an actual density of unity. The many crossings of the curves suggest that energetic flows of highly inhomogeneous fluids would exhibit a complex structure without any definite lattice structure while very slow flows might "freeze" into a least-energy crystalline form. Simulations of the Rayleigh-Bénard problem (convection driven by a temperature gradient in the presence of gravity) support this surmise[7]. Low-energy, high-pressure simulations can actually "freeze", with the smooth particles forming a locked lattice structure rather than flowing. For fluids this freezing

behavior is undesirable. In the next Section we consider the stress-free mechanical stability of the three simplest two-dimensional lattice structures.

III. PHASE INSTABILITY FROM DENSITY POTENTIALS

When discrete particles are involved there can be difficulties in representing the smooth and continuous nature of fluid flows. By analogy with atomistic molecular dynamics, one would expect that regular lattice arrangements of particles would resist shear. In the atomistic case in two space dimensions the shear modulus G is of the same order as the one-particle Hooke's-law force constant evaluated from the Einstein model:

$$G \simeq \kappa_{\rm Einstein} \equiv \frac{\partial^2 \Phi}{\partial x_1^2} \ ,$$

where x_1 is the displacement of a single test particle, Particle 1, from its lattice site, with all the other particles fixed. For a sufficiently simple density-dependent potential we can estimate the one-particle force constant $\kappa_{\rm Einstein}$ analytically.

Let us illustrate for the simplest possible density-dependent potential,

$$\Phi_\rho \equiv \sum_j \frac{1}{2}[\rho_j - \rho_0]^2 \ ; \ \rho_j = \sum_i m_i w_{ij} \ ,$$

where Φ_ρ is the total potential energy of the system, ρ_0 is the target density minimizing that energy, and all the particle masses are set equal to unity, $m_j = 1$. The first derivative,

$$\frac{\partial \Phi_\rho}{\partial x_1} = \sum_j (\rho_1 + \rho_j - 2\rho_0)(xw'/r)_{1j} \ ,$$

vanishes for

$$x_1 = 0 \rightarrow \rho_1 = \rho_j = \rho_0 \ .$$

The second derivative can be estimated by replacing the particle sum with an integral:

$$\frac{\partial^2 \Phi_\rho}{\partial x_1^2} = \sum_j (xw'/r)_{1j}^2 \simeq \int_0^h \left(\frac{xw'}{r}\right)^2 2\pi r dr = \frac{90}{7\pi h^4} \ .$$

Fig. 2 shows that this analytic result closely resembles the detailed lattice sums for all three regular two-dimensional lattices.

Nevertheless, our detailed investigation of this particular choice of fluid model,

$$E = \sum \frac{1}{2}(\rho - \rho_0)^2 \longleftrightarrow P = \rho^2(\rho - \rho_0) \ ,$$

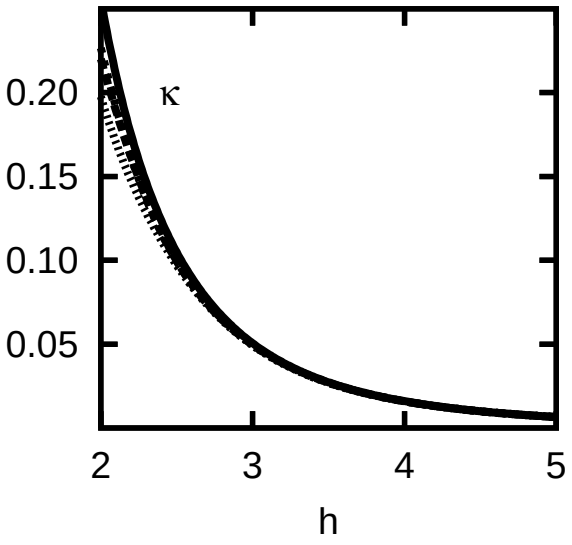

FIG. 2: Comparison of the exact summed-up Einstein force constant $\kappa_{\rm Einstein}$ with the approximate integrated estimate as a function of the range h of Lucy's weight function. The top-to-bottom ordering of the curves is [integrated > triangular > square > hexagonal].

revealed that this expectation of a shear strength varying as h^{-4} is unfounded. Instead, regular lattices, with a stress-free, density-based potential corresponding to an athermal fluid constitutive relation, show no shear resistance whatever, and rapidly "melt"!

Numerical investigation shows that the square, triangular, and hexagonal lattices, arranged *at* the target density ρ_0, are *all* unstable to small displacements. This can be shown by using lattice dynamics, elastic theory, or molecular dynamics. In every case the regular lattices are unstable to a variety of shear modes.

The perfect-crystal elastic constants[8, 9] for this potential can be calculated by two chain-rule differentiations of the potential Φ with respect to the elastic strains:

$$C_{11}V = \frac{\partial^2\Phi}{\partial\epsilon_{xx}^2} \; ; \; C_{12}V = \frac{\partial^2\Phi}{\partial\epsilon_{xx}\partial\epsilon_{yy}} \; ; \; C_{44}V = \frac{\partial^2\Phi}{\partial\epsilon_{xy}^2} \; ;$$

$$\epsilon_{xx} = \frac{\partial u_x}{\partial x} \; ; \; \epsilon_{yy} = \frac{\partial u_y}{\partial y} \; ; \; \epsilon_{xy} = \frac{\partial u_x}{\partial y} + \frac{\partial u_y}{\partial x} \; .$$

Here $u(r) = (u_x, u_y)$ represents an infinitesimal displacement from the perfect-lattice configuration. The resulting elastic constants take the form of lattice sums:

$$C_{11}V = \sum_i \left(\sum_j [x^2(w'/r)]_{ij} \right)^2 \; ;$$

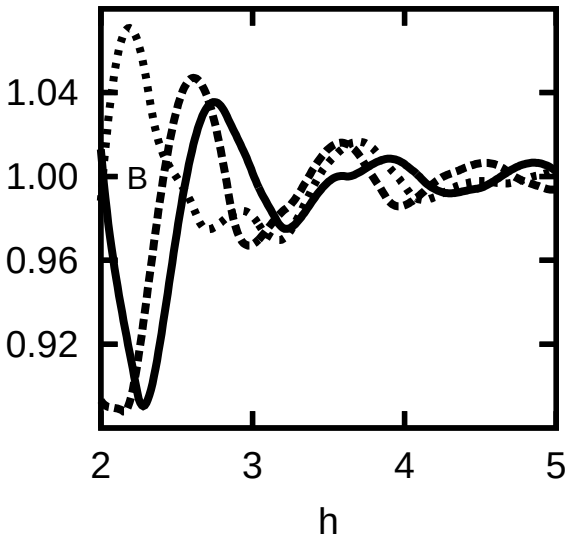

FIG. 3: Variation of the bulk modulus $B = C_{11} + C_{12} = 2C_{11} = 2C_{12}$ with the range of the weight function h for three two-dimensional lattices. The top-to-bottom ordering of the curves at $h = 2.1$ is [hexagonal > square > triangular].

$$C_{12}V = \sum_i \left(\sum_j [x^2(w'/r)]_{ij} \right) \left(\sum_j [y^2(w'/r)]_{ij} \right) \ ;$$

$$C_{44}V = \sum_i \left(\sum_j [xy(w'/r)]_{ij} \right)^2 \ ;$$

$$r_{ij} = \sqrt{x_{ij}^2 + y_{ij}^2} \ ; \ x_{ij} = x_i - x_j \ ; \ y_{ij} = y_i - y_j \ .$$

For the square, triangular, and hexagonal lattices it is evident, by symmetry, that C_{11} and C_{12} are equal and that C_{44} vanishes. Thus these lattices are all unstable to shear. The single nonvanishing elastic constant $C_{11} = C_{12}$ is exactly half the bulk modulus B. The range-dependence $B(h)$ is shown in Fig. 3 for all three lattice structures.

IV. PHASE STABILITY FROM LOCAL DENSITY VARIATION

The results of the preceding section show that the smooth-particle fluid model (correctly) is able to flow under an infinitesimal shear stress. For *solids* shear resistance is required. A simple potential which enhances shear strength minimizes the gradient of the density:

$$\Phi_{\nabla\rho} \propto \sum_j \frac{1}{2} (\nabla\rho)_j^2 \ .$$

This potential is minimized for regular lattices, in which there can (by symmetry) be no density gradient *at* the particle sites. For systems with free surfaces—the details are not considered here, but are elaborated in a forthcoming book[10]—this potential also provides a surface tension, eliminating the tendency of smooth particles to form string-like phases. (Evidently the density gradient is maximized at the "edge" or surface of a condensed phase so that a potential varying as $(\nabla\rho)^2$ minimizes the extent of the surface.)

Figs. 4 and 5 illustrate the enhanced stability of the hexagonal lattice in the absence, and in the presence, respectively of the density-gradient potential. In the one example detailed here (which is typical of many we have investigated, with various sizes, initial conditions, and crystal structures) the individual particle trajectories with and without the density-gradient potential are shown. Evidently, by choosing the proportionality constants wisely, these potentials can be tuned to reproduce desired flow stresses for solids modelled with SPAM. This approach avoids many of the difficulties involved in integrating the smooth-particle equations for the stress rates, $(\{\dot{\sigma}\} \rightarrow \{\sigma\})$.

Interestingly enough, even in the presence of the density-gradient potential, the shear strength vanishes—to see this in the simple case of a square lattice note that simple shear $(\delta x \propto y)$ results in a lattice for which $\Phi_{\nabla\rho}$ still vanishes. In fact the instability can be seen by extending the simulation of Fig. 5 to half a million Runge-Kutta timesteps.

To *guarantee* the stability of the regular lattices an invariant density-*curvature* potential $\Phi_{\nabla\nabla\rho}$ can be constructed:

$$\Phi_{\nabla\nabla\rho} = \tfrac{1}{2}(\rho_{xx} - \rho_{yy})^2 + 2\rho_{xy}^2 \ ;$$
$$\rho_{xx} \equiv \frac{\partial^2\rho}{\partial x^2} \ ; \ \rho_{yy} \equiv \frac{\partial^2\rho}{\partial y^2} \ ; \ \rho_{xy} \equiv \frac{\partial^2\rho}{\partial x \partial y} \ .$$

This potential vanishes for symmetric lattices such as the square, triangular, and hexagonal but ceases to vanish under simple shear, thus stabilizing all those lattices. Detailed numerical work bears this observation out. Because $\Phi_{\nabla\nabla\rho}$ already involves the first and second derivatives of the weight function:

$$(\rho_{xx})_i \equiv \sum_j \left[w' \frac{y^2}{r^3} + w'' \frac{x^2}{r^2} \right]_{ij} \ ,$$

for instance, forces derived from this potential involve the third derivative w'''. Energy can still be accurately conserved provided that a weight function with *three* continuous

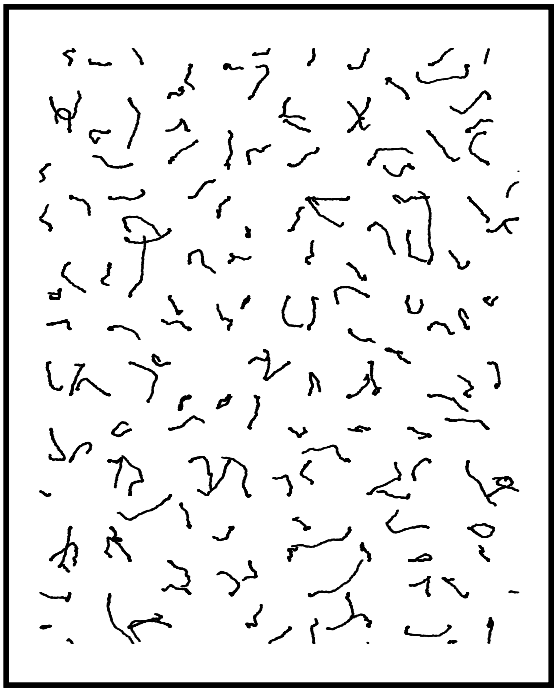

FIG. 4: Hexagonal-lattice particle trajectories *without* the density-gradient potential. Initially the particle displacements were chosen randomly, with zero sum and with an initial rms value of $\sqrt{\langle \delta r^2 \rangle} = 0.02$. The range of Lucy's weight function is $h = 3$ with the density and the particle mass both chosen equal to unity. The elapsed time (40,000 Fourth Order Runge-Kutta timesteps $dt = 0.05$) is about 80 Einstein vibrational periods ($\kappa_{\rm Einstein} \simeq 0.05$). $\Phi_\rho = \frac{1}{2}\sum(\rho - \rho_0)^2$.

derivatives, such as the example given earlier,

$$w_{\rm Smooth}(r < h) = \frac{7}{\pi h^2}\left[1 - \frac{r}{h}\right]^4 \left[1 + 4\frac{r}{h}\right] \ ,$$

is used.

V. CONCLUSIONS

Density-dependent potentials can be used to simulate the behavior of either fluids or solids from the standpoint of smooth-particle simulation. By introducing potentials depending upon the local variation of density, strength and surface tension can be introduced, providing a useful model for solids. Surface tension can also be introduced by using combinations of weight functions with different ranges[5] or by introducing *ad hoc* pair potentials[11]. We

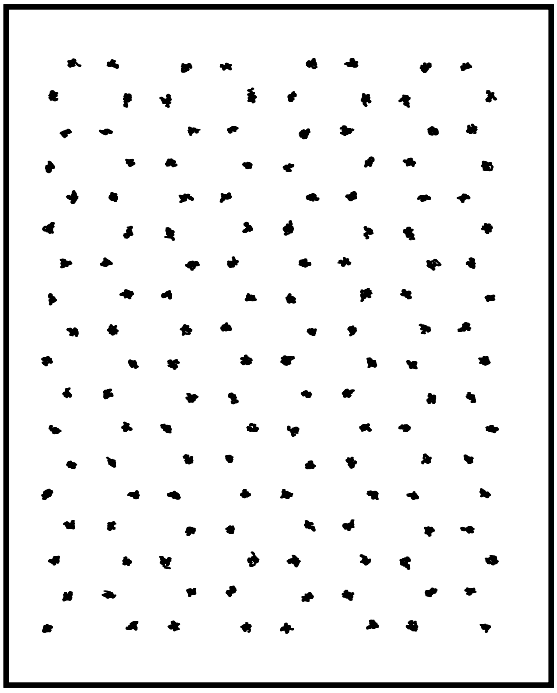

FIG. 5: Hexagonal-lattice particle trajectories *with* the density-gradient potential $\Phi_{\nabla\rho} = \frac{1}{2}\sum(\nabla\rho)^2$. Initial conditions and length of the simulation are identical to those of Figure 4. $\Phi = \Phi_\rho + \Phi_{\nabla\rho} = \frac{1}{2}\sum[(\rho - \rho_0)^2 + (\nabla\rho)^2]$.

think that the present density-based approach has æsthetic advantages over these ideas. We believe that the idea of using density-based potentials will prove fruitful in a wide variety of high-strain-rate applications of smooth-particle methods.

Acknowledgments

Much of this work was carried out with the help of Chris Clark and the support of the Academy of Applied Science's "Research in Engineering Apprenticeship Program" at Great Basin College's High Tech Center during the summer of 2005. Some of the work was performed under the auspices of the United States Department of Energy at the Lawrence Livermore National Laboratory, where we are Participating Guests, under Contract W-7405-Eng-48. We are specially grateful to Mike MacFarlane (Great Basin College) and Bob Ferencz (LLNL) for their help and support. We also thank the anonymous referees for their

thoughtful comments and for bringing Ref. 11 to our attention.

---

[1] L. B. Lucy, The Astronomical Journal **82**, 1013 (1977).

[2] R. A. Gingold and J. J. Monaghan, Mon. Not. R. Astr. Soc. **181**, 375 (1977).

[3] Wm. G. Hoover, Physica A **260**, 244 (1998).

[4] J. W. Swegle, D. L. Hicks, and S. W. Attaway, J. Comp. Phys. **116**, 123 (1995).

[5] S. Nugent and H. A. Posch, Phys. Rev. E **62**, 4968 (2000).

[6] Wm. G. Hoover and C. G. Hoover, Comp. in Sci. Eng. **March/April**, 78 (2001).

[7] O. Kum, Wm. G. Hoover, and H. A. Posch, Phys. Rev. E **52**, 4899 (1995).

[8] D. R. Squire, A. C. Holt, and W. G. Hoover, Physica **42**, 388 (1969).

[9] W. G. Hoover, A. C. Holt, and D. R. Squire, Physica **44**, 437 (1969).

[10] Wm. G. Hoover, "Smooth Particle Applied Mechanics" (World Scientific, Singapore, in preparation, 2005).

[11] A. Tartakovsky and P. Meakin, Phys. Rev. E **72**, 026301 (2005).